Turkish Journal of Electrical Engineering & Computer Sciences

http://journals.tubitak.gov.tr/elektrik/

Research Article

Turk J Elec Eng & Comp Sci
(2018) 26: 895 – 905

doi:10.3906/elk-1706-194

Investigation on optimal parameter selection for LLC half-bridge resonant converter based on FHA

Jianguang MA*, **Xueye WEI**, **Liang HU**, **Wenting JIA**
School of Electronic and Information Engineering, Beijing Jaotong University, Beijing, P.R. China

Received: 16.06.2017 • **Accepted/Published Online:** 24.01.2018 • **Final Version:** 30.03.2018

Abstract: The LLC half-bridge resonant converter has attracted extensive research attention due to its advantages of achieving high efficiency and high power density. However, the resonant process is more complicated, where the main difficulty is to precisely calculate resonant parameters. In this paper, the fundamental harmonic approximation (FHA) method is employed to analyze the resonant process of the converter. In particular, the working mode and the mathematical model of the LLC half-bridge resonant converter are established, where a new method is proposed to determine the operating frequency of LLC based on voltage gain and transformer loss. Based on the proposed method, the converter parameters can be optimized and the drawbacks of manually selecting the frequency can be avoided. Finally, a 200-W LLC converter laboratory prototype is established and the experimental results verify the effects of parameter optimization.

Key words: LLC resonant converter, fundamental harmonic approximation, optimum parameter, resonant parameter

1. Introduction

In recent years, it has become a new requirement and trend to develop high efficiency and high power density in industrial automation, military, aviation, and other equipment miniaturization [1]. DC-DC converters play an important role not only in energy transfer but also in electrical isolation. The increase in operating frequency would decrease the switch power supply and increase the switching losses. In particular, electromagnetic interference produced by high operating frequencies will affect the average performance of the circuit [2].

In the cases of small and medium power, half-bridge topology is simple with fewer components, which has become an important research area. An LLC half-bridge resonant converter can achieve zero-voltage switching (ZVS) and zero-current switching (ZCS) on the primary side of the transformer [3]. It can result in cross losses of the current and voltage in the switching process, which has the characteristics of natural soft switching. It should be noted that the LLC resonant converter working process is rather complicated and that it is often very difficult to establish an accurate model for calculating the resonant parameters. In the fundamental harmonic approximation (FHA) method, the harmonic current of the resonant circuit is used to approximate the fundamental Fourier components, where higher harmonics generated by the switch are neglected. By assuming it to be pure sine waves, resonant converters can be conveniently analyzed with classical AC circuits [4–7].

In the existing literature, LLC resonant converter parameter optimization is in the stage of theoretical development. The resonant voltage gain and the quality factor are the main issues to be considered. Moreover, switching loss can also affect the frequency converter dynamic process. In resonant circuit modal analysis,

*Correspondence: 14111042@bjtu.edu.cn

the proposed parameter optimization method could establish a voltage gain on the basis of the mathematical model, which can be configured by the voltage gain of the resonance parameters [8]. In the gain curve of the LLC resonant converter it is operated in the nonregulated state, where the resonant network could be designed to calculate the loss of the transformer [9]. The LLC resonant model can be established, where parameters selection such as leakage inductance, magnetic inductance, and resonant capacitance can be facilitated based on the efficiency of conversion and the range of load variation. However, this method cannot consider the working range of the switching frequency in the dynamic process of the circuit [10]. To optimize the LLC resonant converter, a control strategy can obtain different loads and different input voltage ranges of the soft switch [11–14].

In this paper, the working mode and the mathematical model of the LLC half-bridge resonant converter are established based on FHA analysis. Based on the optimal voltage gain range and transformer loss, the operating frequency range could be determined, and overall parameters of the converter could be optimized. In this way, the loss of device soft-switching states can be avoided. Finally, the effectiveness of the optimization method is verified by a 200-W laboratory prototype.

2. LLC half-bridge resonant converter

In Figure 1, the LLC half-bridge resonant converter is shown. The input voltage is V_{in}, the two half-bridge MOSFETs are Q_1 and Q_2, and the two MOSFET parasitic capacitors are$coss1$ and $coss2$. In addition, L_s and L_p are the integrated transformer leakage inductance and magnetic inductance, respectively; C_r is the resonant capacitor; a is the transformer turns ratio; D_1 and D_2 are the transformer second side rectifier diodes; C_{out} is the output capacitor; V_{out} is the output voltage; and R is the load.

There are two resonant frequencies for the LLC resonant converter. If only the transformer leakage inductance participates in resonance, the resonant frequency is f_1. If the magnetic inductance participates in resonance, the resonant frequency becomes f_2. The switching frequency of the resonant converter is f_s.

$$f_1 = \frac{1}{2\pi\sqrt{L_s C_r}} \tag{1}$$

$$f_2 = \frac{1}{2\pi\sqrt{(L_s + L_p)Cr}} \tag{2}$$

Figure 2 presents the LLC resonant converter leakage inductance magnetic inductance current and resonant capacitor voltage. In Figure 2, it can be seen that there are three main operating modes for the converter. When the magnetic inductor participates in resonance, the resonant frequency is f_2. The leakage inductor and magnetic inductor current should be equal, i.e. $I(L_p) = I(L_s)$. At this point, the resonant network has not transferred any energy and the transformer output should be zero. If only the leakage inductor and resonant capacitor participate in resonance, the resonant frequency is f_1 when $I(L_p) > I(L_s)$. The magnetic inductor is clamped by voltage $V(L_p) = -aV_{out}$. The resonant network can transfer energy to the secondary switch. It was reported in [14] that the resonant converter operating frequency should meet the condition of $f_2 < f_s < f_1$ to ensure the transformer primary and secondary switches at ZVS and ZCS.

Leakage inductance current can be expressed as:

$$i_{Ls}(t) = \sqrt{2} I_{rms\_p} \sin(\omega t + \theta) \tag{3}$$

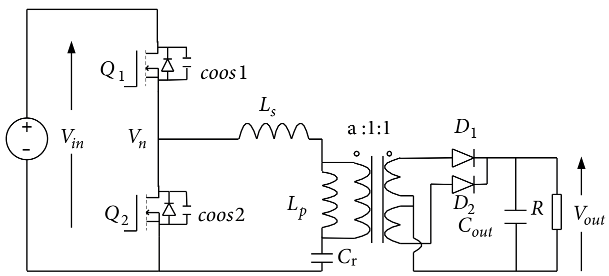

Figure 1. LLC half-bridge resonant converter.

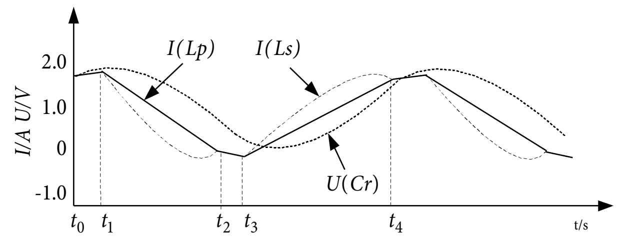

Figure 2. LLC main working waveform.

Magnetic inductance current can be expressed as:

$$i_{Lp}(t) = \frac{aV_{out}}{L_p} \cdot \frac{1}{4f_s} \tag{4}$$

Here, $Vout$ is output voltage, Lp is magnetic inductance, a is ideal transformer turn ratio, and f_s is switch frequency.

The magnetic inductance current should be equal to the leakage inductance current: $i_{Ls}(t) = i_{Lp}(t)$

The output current can be given as:

$$I_O = a\frac{1}{T}\int_0^{\frac{T}{2}} (i_{Ls}(t) - i_{Lp}(t))dt \tag{5}$$

2.1. Circuit model based on FHA

FHA is used for analyzing the LLC resonance, where current and voltage of the resonant network can be approximated by a sine wave with a classical AC circuit. Therefore, the nonlinear circuit in Figure 1 can be converted to the AC linear circuit as in Figure 3.

The resonant network is able to convert DC power to the square wave with frequency f_s, duty cycle 50%, and amplitude V_{in}. The output voltage V_S can be obtained by Fourier decomposition:

$$V_S = \frac{V_{in}}{2} + \frac{2}{\pi}\sum_{n=1,3,5\cdots}\frac{1}{n}\sin(n \cdot 2\pi \cdot f_s \cdot t) \tag{6}$$

The fundamental value of the fundamental components can be given as:

$$u = \frac{\sqrt{2}}{\pi}V_{in} \tag{7}$$

The voltage gain of the LLC half-bridge resonant converter $\|M(j\omega)\|$ can be expressed as:

$$\|M(j\omega)\| = \frac{V_{out}}{V_{in}} \tag{8}$$

The resonant network AC input voltage can be given as:

$$V_S = \frac{2}{\pi}V_{in} \cdot \sin(2\pi \cdot f_s \cdot t + \varphi) \tag{9}$$

Here, φ is the voltage and current phase difference.

After conversion to the primary side, the equivalent resistance can be given as:

$$Re = \frac{8}{\pi^2}a^2R \tag{10}$$

Here, R is the load.

Primary side input current is given as:

$$I_{in} = \frac{2}{\pi}\left\| Is \right\| \cos(\varphi s) = \frac{2}{\pi}\left\| Vs \right\| Re(\frac{1}{Z_i}) \tag{11}$$

Here, I_s is the current RMS value.

The current of resonant converter outputs is given as:

$$I_{out} = \frac{2}{\pi}a\left\| I_R \right\| \tag{12}$$

2.2. LLC equivalent circuit

To facilitate the analysis of the resonant converter voltage gain and input impedance, the LLC resonant circuit given in Figure 1 can be equivalently represented as the circuit shown Figure 4.

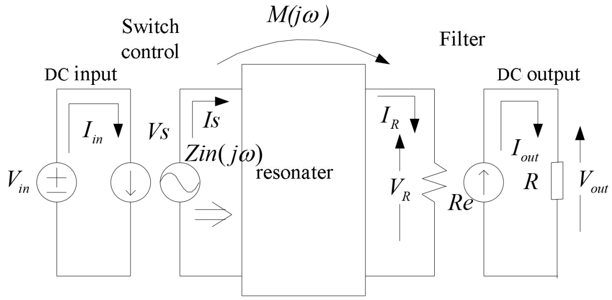

Figure 3. LLC converter FHA model.

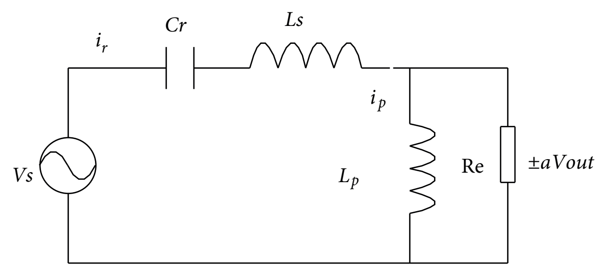

Figure 4. LLC resonant converter equivalent circuit diagram.

Based on Figure 4, the LLC equivalent impedance and voltage gain can be calculated by:

$$Z_{in}(j\omega) = \frac{1}{j\omega C_r} + j\omega L_s + j\omega L_p//Re = \frac{Re(\omega L_p)^2}{(\omega L_p)^2 + Re^2} + j(\frac{Re^2\omega L_p}{(\omega L_p)^2 + Re^2} + \omega Ls - \frac{1}{\omega C_r}) \tag{13}$$

$$M(j\omega) = \frac{j\omega L_p//Re}{z_{in}(j\omega)} = \frac{j\omega L_p//Re}{\frac{Re(\omega L_p)^2}{(\omega L_p)^2+Re^2} + j(\frac{Re^2\omega L_p}{(\omega L_p)^2+Re^2} + \omega Ls - \frac{1}{\omega C_r})} \tag{14}$$

The normalization of the operating frequency can be performed by $x = f_s/f_1$.

Definition: $x < 1$ represents the resonance point below; $x > 1$ represents the resonance point above. The ratio of integrated transformer magnetic inductance and leakage inductance is defined as $k = L_p/L_s$; resonant circuit characteristic impedance is defined as $Z_R = \sqrt{Ls/Cr}$; resonant circuit quality factor is defined as $Q = Z_R/Re$. The quality factor is related to the load. $Q = 0$ indicates $Re = \infty$ (load open circuit) and $Q = \infty$ indicates $Re = 0$ (load short circuit). The input impedance and voltage gain of the resonant circuit can be calculated using the above formula.

3. Voltage gain input impedance analysis and soft-switching implementation

With the three parameters x, k, and Q, the LLC half-bridge resonant converter input impedance Zin and voltage gain M can be obtained as follows [10]:

$$Zin(x,k,Q) = Z_R \cdot \left[Q \cdot \frac{x^2 \cdot k^2}{1+x^2 \cdot k^2 \cdot Q^2} + j \cdot \left(x - \frac{1}{x} + \frac{x \cdot k}{1+x^2 \cdot k^2 \cdot Q^2} \right) \right] \tag{15}$$

$$|M(x,k,Q)| = \frac{1}{2} \cdot \frac{1}{\sqrt{\left[1+\frac{1}{k}\cdot(1-\frac{1}{x^2})\right]^2 + Q^2 \cdot (x-\frac{1}{x})^2}} \tag{16}$$

Based on Eqs. (15) and (16), different quality factors can be obtained under the input impedance curve as shown in Figure 5, and the voltage gain curve as shown in Figure 6.

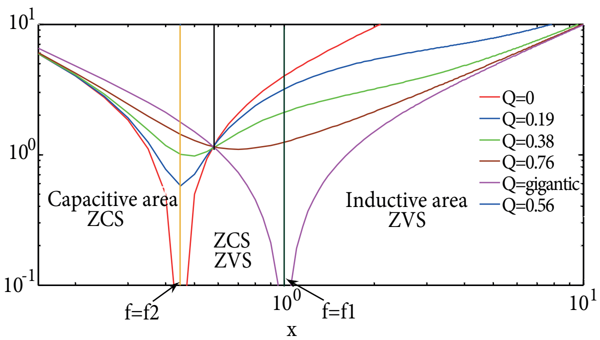

Figure 5. Input impedance.

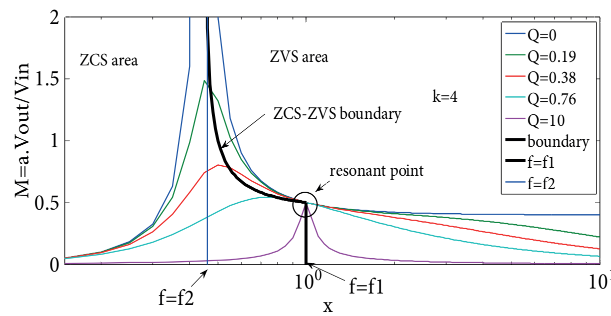

Figure 6. The voltage gain.

1) If $f_s = f_2$, $x = f_2/f_1 = \sqrt{1/(1+k)}$. 2) If $f_s = f_1$, $x = 1$. With different Q values, all the input impedance curves touch at point $x = \sqrt{2/(2+k)}$. 3) If the normalized frequency x represents the quality factor Q, $Q_m(x) = \frac{2\pi^3 f_1 x L_s}{8a^2 R}$. Below the resonance ($\sqrt{\frac{1}{1+k}} < x < 1$), when the input impedance $Zin(j\omega)$ depends on the quality factor $Q_m(x)$, if $Q < Q_m(x)$, the behavior has inductance characteristics of ZVS. If $Q > Q_m(x)$, the behavior has capacitive ZCS. 4) The dividing line of capacitive characteristics and inductance characteristics should depend on $Im(Zin(j\omega)) = 0.5$), where $|Zin(j\omega)|$ is proportional to the load if $x > \sqrt{\frac{2}{2+k}}$. A smaller load often leads to a smaller input current, where $|Zin(j\omega)|$ is inverse proportional to the load with $x < \sqrt{\frac{2}{2+k}}$. A smaller load will result in a larger input current.

In Figure 6, the voltage gain curve of the LLC resonant circuit is presented under different quality factors. Under different quality factors, all the voltage gain curves should be subject to independent resonant points $x = 1$, $M = 0.5$. The output open circuit curve ($Q = 0$) is above the ZVS–ZCS boundary, $M = \frac{k}{2(1+k)}$, if $x \to \infty$; when $M \to \infty$ then $x = \sqrt{\frac{1}{1+k}}$. All extreme points are in the region of capacitance characteristics. Voltage gain is $M < 0.5$ if the resonance point is above $x > 1$. In contrast, voltage gain is $M > 0.5$ if the resonance point is below $x < 1$.

In the case of a fixed value ($Q = 0.38$), the voltage gain curves for the different values are shown in Figure 7. The value is the ratio of the integrated transformer magnetic inductance and leakage inductance. It can be seen from this figure that greater voltage gain k in the vicinity of the frequency $x = 1$ will lead to a smaller rate of change. Although higher voltage gain is often more desirable, overly large values will inevitably cause the feedback system to overshoot. Moreover, difficulties of the transformer design will occur when the value becomes too large or too small. In the circuit design, the usual value selection range should be $2 < k < 7$.

By switching frequency, the LLC half-bridge resonant converter is able to regulate the voltage gain M to obtain adjustment of output voltage. Its range is $f_{\min} < f_s < f_{\max}$. The form of normalized frequency can be expressed as $x_{\min} < x < x_{\max}$. It can be seen from Figure 8 that the resonant converter voltage gain is step-down, step-up, and 1 when $M < 0.5$, $M > 0.5$, and $M = 0.5$, respectively. If the frequency is in the range of $f_s \sim f_2$, the converter is in the region of capacitance characteristics.

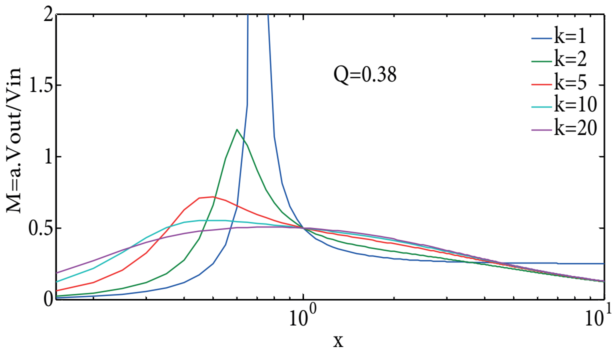

Figure 7. Voltage gain of different k values.

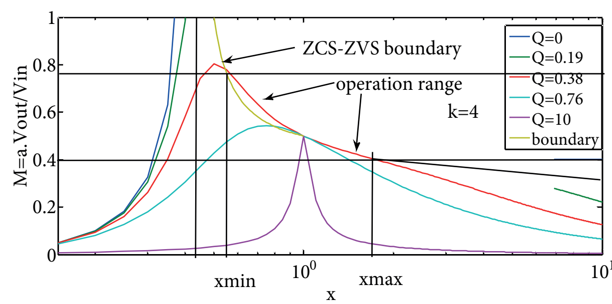

Figure 8. Operating area frequency range.

4. Loss analysis

To obtain optimized parameters for improving the efficiency of an LLC resonant converter, accurately calculating the various parts of the loss is necessary. In particular, the main losses should consist of MOSFET turn-off loss, integrated transformer losses, rectifier conduction losses, capacitor ESR loss, and wire loss. Due to the characteristics of the soft switch, the conduction loss of the switch should not be considered any longer. The analysis of MOSFET turn-off loss and integrated transformer loss will be given as follows.

It is well known that the MOSFET gate-source equivalent capacitance is constant, whereas the values of gate-drain and the drain-source equivalent capacitance are dynamical, which are related to the voltage in the MOSFET. A half-bridge circuit has two MOSFETs, where the equivalent capacitance are $coss1$ and $coss2$, where the relationship between the equivalent capacitor and MOSFET voltage is shown in Eq. (17).

$$\frac{coss(V_{DS1})}{coss(V_{DS2})} \approx \sqrt{\frac{V_{DS2}}{V_{DS1}}} \tag{17}$$

The equivalent capacitance is often provided by the MOSFET manufacturer, which can be calculated under the conditions of $V_{DS} = 25\, V_{GS} = 0$, as given in Eq. (18).

$$coss(V_{DS}) = coss25\sqrt{\frac{25}{V_{DS}}} = \frac{5coss25}{\sqrt{V_{DS}}} \tag{18}$$

In general, the equivalent capacitance of the MOSFET plays two different roles in the switching process. The stored energy from the MOSFET conduction process in the $coss$ will be dissipated in the MOSFET on-resistance R_{DS}, which is the conduction capacitor loss. In contrast, the MOSFET can work in the ZVS in the LLC resonant circuit, where capacitance loss can be ignored. In the MOSFET, turning off the process of equivalent voltage on the capacitor leads to the overlap area of MOSFET current and voltage. This can be considered as switching loss, which cannot be ignored in the LLC resonant circuit. The MOSFET heat that causes it is derived from this turn-off loss. C_{stray} is the stray capacitance in the resonator, where the equivalent capacitance and stray capacitance of the two MOSFETs are shown in Figure 9. The two MOSFETs are equivalent to the capacitive capacitance of the stray capacitance C_{stray} and the half-bridge midpoint equivalent capacitance C_{HB}, and the equivalent capacitance C_{HB} is much smaller than the resonant capacitor C_r.

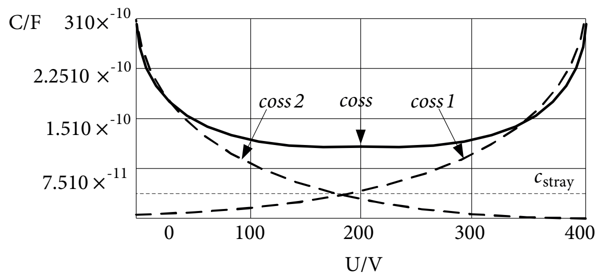

Figure 9. The relationship between the equivalent capacitance of the MOSFET and the midpoint voltage of the half-bridge.

$$C_{HB} = C_{Stray} + 2\sqrt{\frac{V_{DSS}}{V_{in}}}coss \tag{19}$$

Since the half-bridge midpoint equivalent capacitance C_{HB} structure is complicated, an equivalent linear capacitor is used for computational convenience, where the half-bridge midpoint voltage is V_{HB} and flow through the capacitor current is I_{CHB}. Therefore, the Q_2 of loss energy $E_{off}(Q_2)$ and power $P_{off}(Q_2)$ can be expressed as:

$$I_{C_{HB}}(t) = C_{HB}\frac{dV_{HB}}{dt} \tag{20}$$

$$V_{HB}(t) = \frac{1}{C_{HB}}\int_0^t I_{C_{HB}}(t)dt = \frac{1}{C_{HB}}\int_0^t [I_{R0} - I_{Q2}(t)]dt \tag{21}$$

$$E_{off}(Q_2) = \int_0^{T_f} I_{Q2}(t)V_{HB}(t)dt = \frac{(I_{R0}\cdot T_f)^2}{24C_{HB}} \tag{22}$$

$$P_{off}(Q_2) = E_{off}(Q_2)f_{sw} \tag{23}$$

The two MOSFETs are symmetrical in the circuit, where the total turn-off loss can be given as:

$$P_{off}(MOS) = 2E_{off}(Q_2)f_s = \frac{(I_{R0}\cdot T_f)^2}{12C_{HB}}f_s \tag{24}$$

In Figure 9, the MOSFET equivalent capacitance and half-bridge midpoint voltage relationship is given. It can be seen from Eq. (24) that in the half-bridge there is two-MOSFET turn-off loss with four parameters.

5. Experiment results and analysis

In this experiment, the design method of the frequency range of the LLC resonant converter is to be verified based on the voltage gain and the transformer loss. For this purpose, a test prototype with an input of 380 V and an output of 120 V and 200 W is designed. In Table 1, the design and selection of the resonant circuit parameters are shown, and in Table 2, the test device used in the power device is given.

Table 1. LLC resonant converter component parameters.

Parameters	Values
Input voltage V_{in}	380–400 V
Output voltage V_{out}	120 V
Resonant frequency f_s	200 kHz
Minimum switching frequency f_2	136 kHz
Resonant capacitor C_r	15 nF
Resonance inductance L_s	25 μH
Magnetic inductance L_p	124 μH
Magnetic inductance and leakage inductance ratio	5
Dead time	330 ns
Transformer turns ratio a	1.5

Table 2. LLC resonant converter component parameters.

Device	Model
Integrated transformer	PQ35
MOSFET Q_1, Q_2	2SK3934
Rectifier diode D_1, D_2	STTH12R06D
Drive chip	IR2110

In Figure 10, the LLC resonant half-bridge is shown with the dead zone of the upper and lower duty cycle of the complementary MOSFET switch waveform. In Figure 10a, the driving signal waveforms of Q_1 and Q_2 are shown where the fixed duty cycle is 50% and dead time is 330 ns. In Figure 10b, the drive waveform and conduction waveform of Q_1 are also given. The two figures show that Q_1 and Q_2 can achieve ZVS on the primary side.

In Figure 11, the sinusoidal voltage waveforms of resonant capacitor C_r are shown. Resonant capacitors can not only participate in the resonance of the LLC resonator but can also play an important role in preventing the magnetic saturation of the integrated transformer. The measured resonant capacitor voltage waveform is consistent with that of the model, as shown in Figure 2, which can validate the effectiveness of the proposed method.

In Figure 12, the primary and secondary voltage waveforms of the integrated transformer are presented. It can be seen from Figure 12a that the resonant point can be observed if the current of leakage inductance equals the current of magnetic inductance. The experimental results have shown that the proposed method can determine the optimized operating frequency of the parameter based on the converter voltage gain and the transformer loss. The converter primary voltage zero conduction can be obtained. In Figure 12b, the

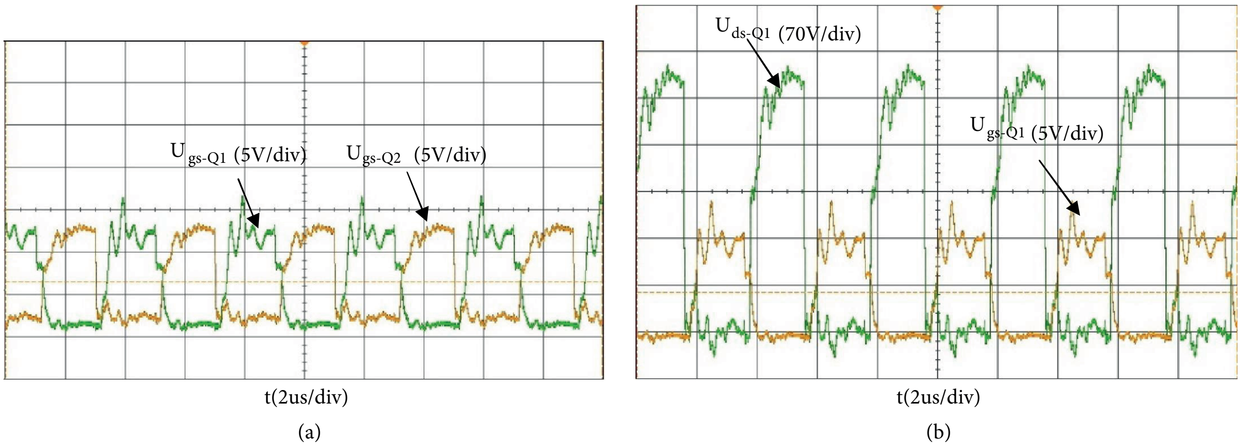

Figure 10. (a) Q_1, Q_2 drive waveform; (b) Q_1 drive and conduction waveform.

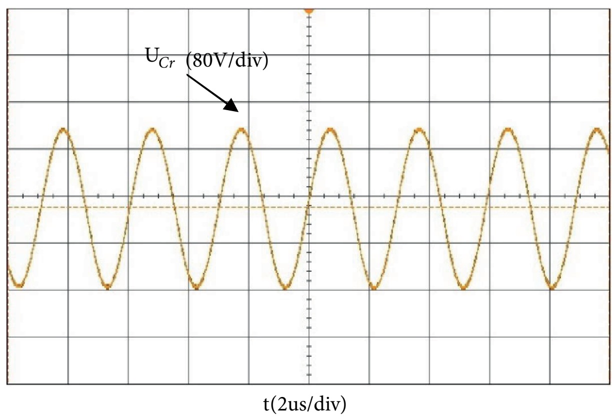

Figure 11. Resonant capacitor voltage waveform.

secondary voltage waveform of the integrated transformer with center-tapping can be observed. In particular, the secondary side rectifier diode turned OFF with ZCS is near the resonance point.

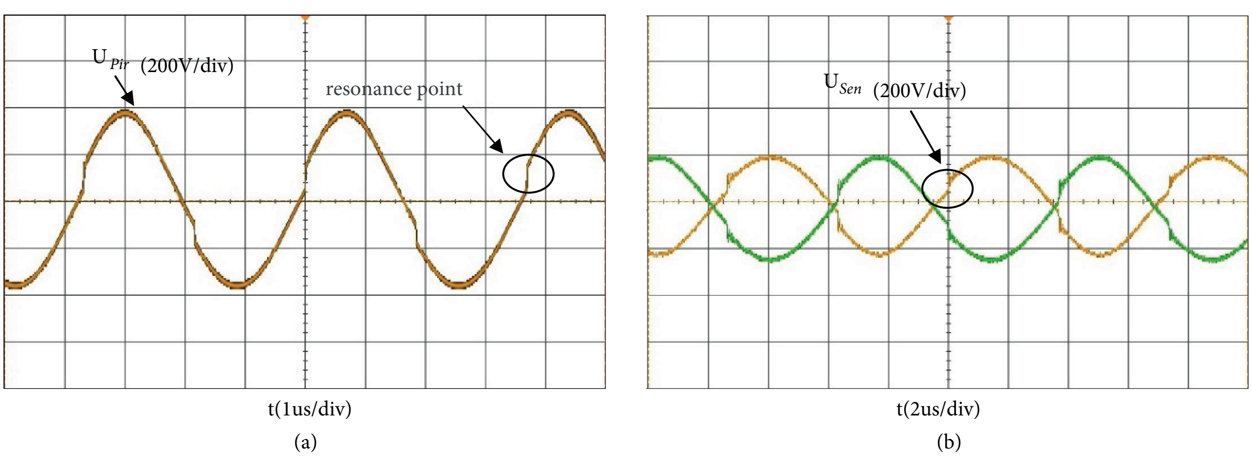

Figure 12. (a) Primary side waveform; (b) secondary side waveform.

The LLC resonant converter normal output voltage is shown in Figure 13, where the input voltage is 380 V, the output voltage is 120 V, the full load current is 1.6 A under the conditions of the output voltage waveform, and the peak of ripple is approximately 300 mV. A reasonable selection of the resonant circuit parameters can control the ripple of the output voltage.

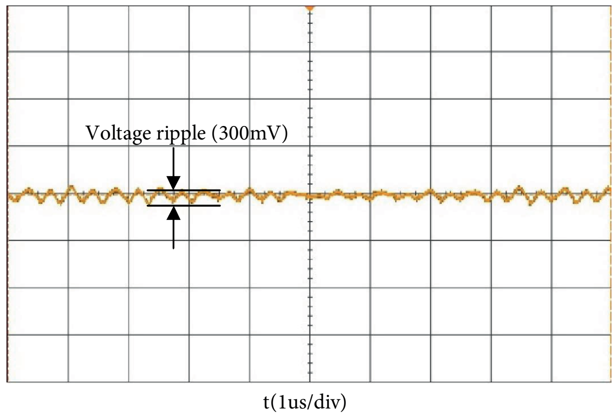

Figure 13. The output voltage.

In Figure 14, the measured efficiency curve is shown in terms of the rated output voltage of the resonant converter. This curve demonstrates that the proposed parameter design method can constrain the resonant converter more than 70% with a wide output load from 30 W to 200 W, where the highest efficiency can achieve 95%. Figure 15 shows the experimental prototype for the proposed FHA analysis method.

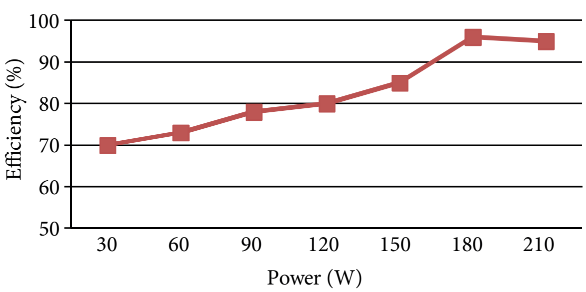

Figure 14. Measured efficiency curve versus rated output power.

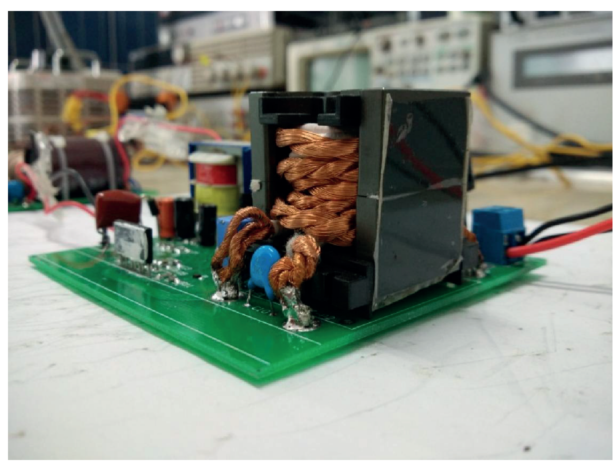

Figure 15. Photo of the experimental prototype.

6. Conclusion

The LLC converter model can be established by FHA, where the optimal operating frequency of the LLC converter can be determined. Based on FHA, a new method is proposed to optimize LLC resonant converter parameters by configuring the optimal voltage gain and integrated transformer loss. In this way, the operating frequency range can be determined and the converter can operate in its optimum state.

Three types of working modes of LLC resonant converter are analyzed, where mathematical models can be established. The input impedance and voltage gain are quantitatively analyzed and soft switching is implemented in a resonant circuit under different load conditions. Based on the proposed method, a prototype is built and used for verification. Finally, the effectiveness of the optimization method is verified by a 200-W laboratory prototype. The experimental results have shown that the proposed method is rather effective.

References

[1] Hu ZY, Qiu YJ, Wang LI, Liu YF. An interleaved LLC resonant converter operating at constant switching frequency. IEEE T Power Electr 2014; 29: 2931-2944.

[2] Lee JB, Kim JK, Kim JH, Baek JI, Moon GW. A high-efficiency PFM half-bridge converter utilizing a half-bridge LLC converter under light load conditions. IEEE T Power Electr 2015; 30: 4931-4943.

[3] Beiranvand R, Rashidian B, Zolghadri MR, Alavi SMH. A design procedure for optimizing the LLC resonant converter as a wide output range voltage source. IEEE T Power Electr 2012; 27: 3749-3764.

[4] Yu RY, Ho GKY, Pong BMH, Ling BWK, Lam J. Computer-aided design and optimization of high-efficiency LLC series resonant converter. IEEE T Power Electr 2012; 27: 3243-3257.

[5] Wang CF, Xu QC. Study of LLC resonant converter for variable-frequence microwave oven power supply. Transactions of China Electrotechnical Society 2012; 27: 103-110 (in Chinese with English abstract).

[6] Yuan YS, Luo F, Hu PA. One bridge-type secondary-side LLC resonant DC-DC converter. Proceedings of the CSEE 2014; 34: 6415-6426 (in Chinese with English abstract).

[7] Zheng RC, Liu BY, Duan SX. Analysis and parameter optimization of start-up process for LLC resonant converter. IEEE T Power Electr 2015; 30: 7113-7123.

[8] Beiranvand R, Rashidian B, Zolghadri MR, Alavi SMH. Optimizing the normalized dead-time and maximum switching frequency of a wide-adjustable-range LLC resonant converter. IEEE T Power Electr 2011; 26: 462-472.

[9] Fang X, Hu HB, Chen F, Somani U, Auadisian E, Shen J, Batarseh I. Efficiency-oriented optimal design of the LLC resonant converter based on peak gain placement. IEEE T Power Electr 2013; 28: 2285-2296.

[10] Fang X, Hu HB, Chen F, Somani U, Auadisian E, Shen J, Batarseh I. Operation mode analysis and peak gain approximation of the LLC resonant converter. IEEE T Power Electr 2012; 27: 1985-1995.

[11] Ivensky G, Bronshtein S, Abramovitz A. Approximate analysis of resonant LLC DC-DC converter. IEEE T Power Electr 2011; 26: 3274-3284.

[12] Lo YK, Lin CY, Hsieh MT, Lin CY. Phase-shifted full-bridge series-resonant DC-DC converters for wide load variations. IEEE T Ind Electron 2011; 58: 2572-2575.

[13] Shafiei N, Ordonez M, Craciun M, Botting C, Edington M. Burst mode elimination in high power LLC resonant battery charger for electric vehicles. IEEE T Power Electr 2016; 31: 1173-1188.

[14] Wang HL, Chen Y, Liu YF, Afsharian J, Yang JH. A passive current sharing method with common inductor multiphase LLC resonant converter. IEEE T Power Electr 2017; 32: 6994-7010.